

# A new finite volume method incorporating radial basis functions for simulating diffusion

T. J. Moroney\*      I. W. Turner†

13 September 2004

## Abstract

The finite volume method is the favoured numerical technique for solving (possibly coupled, nonlinear, anisotropic) diffusion equations. The method transforms the original problem into a system of nonlinear, algebraic equations through the process of discretisation. The accuracy of this discretisation determines to a large extent the accuracy of the final solution.

A new method of discretisation is presented, designed to achieve high accuracy without imposing excessive computational requirements. In particular, the method employs radial basis functions as a means of local gradient interpolation. When combined with high order Gaussian quadrature integration methods, the interpolation based on radial basis functions produces an efficient and accurate discretisation.

The resulting nonlinear, algebraic system is solved efficiently using a Jacobian-free Newton-Krylov method. Information obtained from the Newton-Krylov iterations is used to construct an effective preconditioner in order to reduce the number of nonlinear iterations required to achieve an accurate solution.

Results to date have been promising, with the method giving accuracy several orders of magnitude better than simpler methods based on shape functions.

---

\*School of Mathematical Sciences, Queensland University of Technology, Brisbane, AUSTRALIA.  
<mailto:t.moroney@qut.edu.au>

†School of Mathematical Sciences, Queensland University of Technology, Brisbane, AUSTRALIA.  
<mailto:i.turner@qut.edu.au>

# Contents

<b>1</b>	<b>Introduction</b>	<b>2</b>
<b>2</b>	<b>Finite volume method</b>	<b>3</b>
<b>3</b>	<b>Gaussian quadrature</b>	<b>4</b>
<b>4</b>	<b>Interpolation</b>	<b>4</b>
4.1	Shape functions . . . . .	5
4.2	Radial basis functions . . . . .	5
4.2.1	Gradient evaluation . . . . .	6
4.2.2	Improving accuracy near boundaries . . . . .	6
<b>5</b>	<b>Solution of nonlinear system</b>	<b>7</b>
5.1	Preconditioning . . . . .	7
<b>6</b>	<b>Numerical experiments</b>	<b>7</b>
6.1	Test problem . . . . .	7
6.2	Results and discussion . . . . .	8
<b>7</b>	<b>Conclusions</b>	<b>9</b>

## 1 Introduction

The finite volume method is a numerical method for solving partial differential equations. It is particularly well suited for problems involving diffusion [6]. For these problems, an integral involving the diffusive flux component must be evaluated numerically. This requires both a means of numerical integration, and a means of gradient approximation at the integration points. The accuracy of these two components has a large bearing on the overall accuracy of the finite volume method.

We investigate the effectiveness of using radial basis functions as a means of interpolation, coupled with Gaussian quadrature as a means of numerical integration. This approach can result in highly accurate finite volume discretisations, meaning that accurate solutions can be obtained using a much coarser mesh than is possible when using simpler discretisation methods.

By using the method of radial basis functions in combination with shape function-based methods, an accurate solution can be obtained in fewer iterations. Furthermore, the method of shape functions can provide useful information that can be used to precondition the underlying linear system based on radial basis functions.

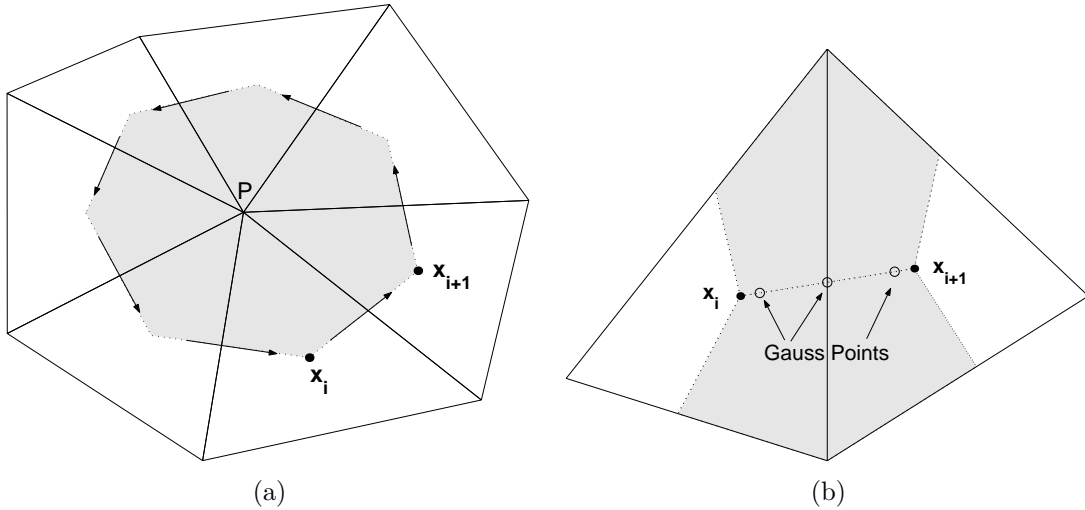


Figure 1: (a) Forming control volumes by joining element centroids. (b) Three-point gaussian quadrature over a control volume face

Some numerical experiments are presented that demonstrate the high accuracy of the new method, giving solutions up to three orders of magnitude more accurate than those obtained using shape functions.

## 2 Finite volume method

The finite volume method is based on a discretisation of the original partial differential equation. To this end, it employs a mesh—a geometric structure consisting of a set of nodes, and the corresponding connections between these nodes to form elements. In this work, the mesh generation software *EasyMesh* (available online from <http://www-dinma.univ.trieste.it/~nirftc/research/easymesh/>) was used to generate an unstructured, triangular mesh.

The finite volume method discretises the original conservation law by forming so-called *control volumes* around each node in the mesh and integrating over each control volume to produce a set of discrete function values at the nodes. Figure 1(a) shows how the control volumes are formed by joining element centroids.

To illustrate the finite volume discretisation strategy, consider the following steady-state diffusion equation

$$\nabla \cdot (\mathbf{D}\nabla\varphi) + S = 0. \quad (1)$$

This partial differential equation is transformed into two-dimensional control-volume

form by integrating over each control volume  $V_P$  and applying the divergence theorem

$$\sum_{i=0}^{n-1} \int_{\mathbf{x}_i}^{\mathbf{x}_{i+1}} \mathbf{D}\nabla\varphi \cdot \hat{\mathbf{n}} \, ds + \Delta A_P \bar{S} = 0 \quad (2)$$

where  $\bar{S} = \frac{1}{\Delta A_P} \int_{V_P} S \, dV$  is the volume average of  $S$ . Equation (2) is exact since no approximation has been made to this point of the derivation. Solving this equation requires approximating the line integral  $\int_C \mathbf{D}\nabla\varphi \cdot \hat{\mathbf{n}} \, ds$  using an appropriate quadrature rule. The accuracy of this approximation has a large bearing on the overall accuracy of the finite volume method. In this work, we investigate using high order quadrature methods.

### 3 Gaussian quadrature

Numerical quadrature methods approximate the integral in (2) by a sum of weights times integrand values. Here a three-point Gaussian quadrature rule is used [4],

$$\int_{\mathbf{x}_i}^{\mathbf{x}_{i+1}} \mathbf{D}\nabla\varphi \cdot \hat{\mathbf{n}} \, ds \approx \sum_{j=1}^3 w_j [\mathbf{D}\nabla\varphi \cdot \hat{\mathbf{n}}]_{\mathbf{x}_j} \quad (3)$$

using the the parameterisation

$$\mathbf{x}(t) = \frac{1}{2}(1-t)\mathbf{x}_i + \frac{1}{2}(1+t)\mathbf{x}_{i+1}, \quad -1 \leq t \leq 1. \quad (4)$$

This three-point scheme is applied over the length of the control volume face as illustrated in Figure 1(b). It can be shown [4] that whereas the midpoint rule is  $\mathcal{O}(h^2)$ , three-point Gaussian quadrature is  $\mathcal{O}(h^6)$ , where  $h$  is the length of (in this case) the control volume face.

### 4 Interpolation

To compute the line integral (3) using the three-point Gaussian quadrature technique outlined in Section 3, the values of the integrand  $\mathbf{D}\nabla\varphi \cdot \hat{\mathbf{n}}$  are needed at points on the control volume face. Recall that as a result of the finite volume discretisation, only the values of  $\varphi$  are available at the node points in the mesh. These values must be used to reconstruct the required gradient  $\nabla\varphi$  at the control volume face. We discuss two methods to achieve this: the well-known shape function method, and a novel method based on radial basis functions.

## 4.1 Shape functions

A popular method of interpolation in the finite volume literature is borrowed from finite element theory. The method of *shape functions* uses the values of  $\varphi$  on the three vertices of a triangular element to compute a constant interpolation of  $\nabla\varphi$  within the element, given by [3]

$$\nabla\varphi = \sum_{i=1}^3 N_i\varphi_i. \quad (5)$$

Finite volume methods that employ these shape functions are often called control volume-finite element, or CV-FE, methods. For problems where the gradient does not vary greatly over small regions this approach can be satisfactory. However, in many problems, there are regions where the gradient can vary significantly and using shape functions will not adequately capture this behaviour.

Some work has been done (see for example [6]) on extending CV-FE methods of flux approximation to second and higher orders of accuracy. Typically, a least-squares approach is used to formulate a higher-degree interpolating polynomial. Rather than extend or improve on this work, it was decided here to investigate alternative methods of interpolation that might also yield high-order gradient approximations.

## 4.2 Radial basis functions

The method of radial basis functions, or RBFs, is a scattered data interpolation method in  $\mathbb{R}^n$ . Given a set of nodes  $\{\mathbf{x}_1, \mathbf{x}_2, \dots, \mathbf{x}_N\}$  and the corresponding function values  $\{\varphi_1, \varphi_2, \dots, \varphi_N\}$ , the RBF interpolating function  $s$  is given by

$$s(\mathbf{x}) = \sum_{j=1}^N \lambda_j \phi(\|\mathbf{x} - \mathbf{x}_j\|) + \sum_{k=0}^{\dim(\pi_m^n)} c_k p_k(\mathbf{x}) \quad (6)$$

where the  $\lambda_j$  and  $c_k$  are determined by the conditions

$$s(\mathbf{x}_j) = \varphi(\mathbf{x}_j), \quad j = 1, 2, \dots, N \quad (7)$$

and

$$\sum_{j=1}^N \lambda_j p_k(\mathbf{x}) = 0, \quad k = 0, 1, \dots, \dim(\pi_m^n) \quad (8)$$

where  $\pi_n^m$  denotes the space of all polynomials in  $n$  variables up to degree  $m$  and the  $p_k$  are the standard basis polynomials for this space. The choices for  $\phi(r)$  used in this study are the thin plate spline,  $\phi(r) = r^2 \log(r)$  and the multiquadric,  $\phi(r) = \sqrt{c^2 + r^2}$ . Based on numerical experimentation, the degree of the polynomial term, and the parameter  $c^2$  are both taken to be 3.

### 4.2.1 Gradient evaluation

It is shown in [9] that the function  $s$  of (6) is differentiable for both the thin plate spline and the multiquadric on any region of  $\mathbb{R}^n$  that excludes the interpolation points. Thus from (6),  $\nabla s$  is given by

$$\nabla s = \sum_{j=1}^N \lambda_j \left( \frac{\mathbf{x} - \mathbf{x}_j}{\|\mathbf{x} - \mathbf{x}_j\|} \right) \phi'(\|\mathbf{x} - \mathbf{x}_j\|) + \sum_{k=1}^n c_k \mathbf{e}_k. \quad (9)$$

### 4.2.2 Improving accuracy near boundaries

It is well known that the accuracy of RBF-based interpolations is poorest near the convex hull of the set of nodes [5]. We overcome this problem in two ways:

1. Using one interpolation per element, as with shape functions
2. Incorporating boundary information into the interpolation

The method of shape functions fits a function  $s$  that is valid only over a given triangular element. We take the same approach when using radial basis functions, and fit one function per element. Each function  $s$  incorporates only a small proportion of the total number of nodes. In this way, points of evaluation do not lie on or near the convex hull of the set, with the exception of points on or near the domain boundary itself. This approach also ensures the nonlinear method of Section 5 operates on a sparse matrix.

To further improve the accuracy of the interpolation, we modify the standard RBF formulation (6) so that boundary nodes include information available from the corresponding boundary condition. For example, the following boundary condition represents Newtonian heat conduction with an external temperature  $\varphi_\infty$ :

$$-\mathbf{D}\nabla\varphi \cdot \hat{\mathbf{n}} = h(\varphi - \varphi_\infty). \quad (10)$$

At boundary nodes, this equation provides information about the behaviour of  $\nabla\varphi$ . To make use of this information, we include an extra term in (6) using a second radial basis function  $\phi_2$ , which we take as the thin plate spline, (and we will now refer to the first, which we take as the multiquadric, as  $\phi_1$ ). Assuming the first  $M$  nodes are boundary nodes with a boundary condition such as (10), the new form for  $s$  is:

$$s(\mathbf{x}) = \sum_{j=1}^N \lambda_j \phi_1(\|\mathbf{x} - \mathbf{x}_j\|) + \sum_{j=1}^M \gamma_j \phi_2(\|\mathbf{x} - \mathbf{x}_j\|) + \sum_{k=0}^{\dim(\pi_m^n)} c_k q_k(\mathbf{x}) \quad (11)$$

where in addition to (7) and (8) we impose

$$\nabla s(\mathbf{x}_j) \cdot \hat{\mathbf{n}} = \nabla\varphi(\mathbf{x}_j) \cdot \hat{\mathbf{n}}, \quad j = 1, 2, \dots, M. \quad (12)$$

## 5 Solution of nonlinear system

In the general nonlinear case, equation (2), when approximated using the techniques of Sections 3 and 4, is the  $P$ th co-ordinate function of a nonlinear system

$$\mathbf{F}(\boldsymbol{\varphi}) = \mathbf{0} \quad (13)$$

which must be solved to obtain the solution  $\boldsymbol{\varphi} = (\varphi_1, \varphi_2, \dots, \varphi_N)^T$ . A Jacobian-free Newton-Krylov method utilising GMRES-DR [8] is used to solve this system. The solution is obtained in three stages, using three different interpolation strategies in the evaluation of  $\mathbf{F}$ :

1. Shape functions
2. Radial basis functions without additional boundary information
3. Radial basis functions with additional boundary information

The reason for this three-stage process is to first make use of the much cheaper shape functions to generate a solution of reasonable accuracy. This solution is then “corrected” using radial basis functions. The two stages of RBFs are necessary to ensure the solution is highly accurate before boundary information is introduced. Failure to do so may lead to divergence since in (12) it is assumed that exact boundary information is available.

### 5.1 Preconditioning

Two preconditioners are used in combination. The first is a matrix of specified sparsity minimising  $\|\mathbf{I} - \mathbf{J}\mathbf{M}_1\|_F$ , where  $\mathbf{J}$  is the Jacobian matrix, as discussed in [2]. The second is the deflation matrix  $\mathbf{M}_2$  discussed in [1] that takes eigenvalue information from GMRES-DR and forms a matrix that explicitly deflates the smallest  $k$  eigenvalues from  $\mathbf{J}$ . The majority of the work in forming these two preconditioners can be done in Stage 1 of the nonlinear process, under the assumption that the Jacobian matrices in all three stages will share similar eigenvalue properties. The preconditioners are used in combination on the right, giving the underlying linear system

$$(\mathbf{J}\mathbf{M}_1\mathbf{M}_2)(\mathbf{M}_2^{-1}\mathbf{M}_1^{-1}\boldsymbol{\delta}\boldsymbol{\varphi}) = -\mathbf{F}. \quad (14)$$

## 6 Numerical experiments

### 6.1 Test problem

The test problem is the classical steady-state heat diffusion equation

$$\nabla \cdot (\mathbf{D}\nabla\mathbf{u}) = -g_0. \quad (15)$$

Table 1: Parameter values for numerical experiments

Parameter	Description	Value
$D_{xx}$	Thermal diffusivity in x direction	$5.0 \text{ m}^2 \text{ s}^{-1}$
$D_{yy}$	Thermal diffusivity in y direction	$5.0 \times 10^i \text{ m}^2 \text{ s}^{-1}$
$g_0$	Source	$10.0 \text{ K m}^{-2} \text{ s}^{-1}$
$h$	Heat transfer coefficient	$2.0 \text{ W m}^{-2} \text{ K}^{-1}$
$\varphi_\infty$	External temperature	$20.0 \text{ K}$
$a$	Length in x direction	$1.0 \text{ m}$
$b$	Length in y direction	$1.0 \text{ m}$

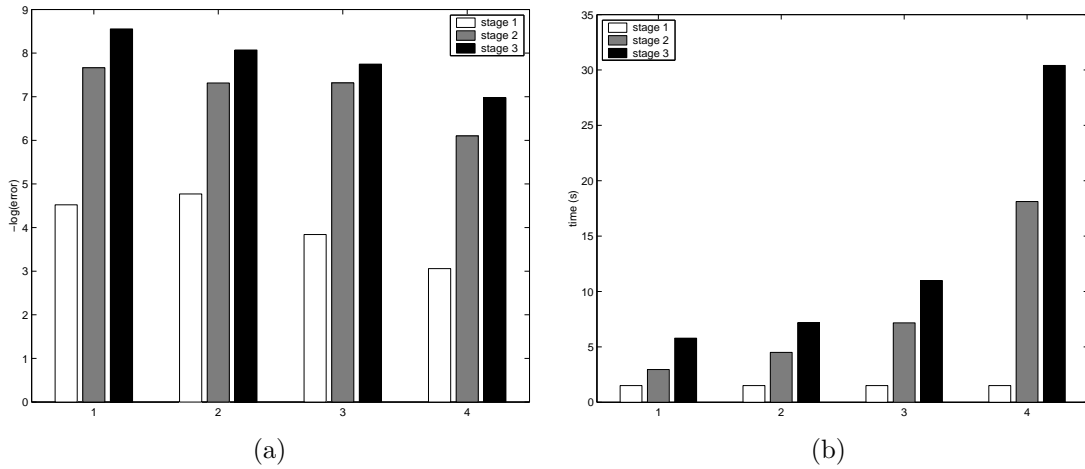


Figure 2: (a) Error in solution after each stage. (b) Cumulative time taken for each stage. 1:  $D_{yy}/D_{xx} = 1$ . 2:  $D_{yy}/D_{xx} = 10$ . 3:  $D_{yy}/D_{xx} = 100$ . 4:  $D_{yy}/D_{xx} = 1000$ .

with constant diffusion tensor  $\mathbf{D} = \text{diag}(D_{xx}, D_{yy})$  and constant source  $g_0$ , on the rectangular domain  $0 \leq x \leq a$ ,  $0 \leq y \leq b$ . The boundaries  $x = 0$  and  $y = 0$  are taken to be insulated, and the boundaries  $x = a$  and  $y = b$  to be subject to Newtonian cooling with external temperature  $\varphi_\infty$ . The analytic solution of this problem is given in [7]. The parameter values used in the experiments are given in Table 1. The parameter  $D_{yy}$  was varied from 5 to 5000 to provide an increasingly challenging problem numerically. A mesh of 236 triangular elements was used with the finite volume method.

## 6.2 Results and discussion

Figure 2(a) shows the accuracy of the numerical solution after each of the three stages of the Newton-Krylov method discussed in Section 5. The relative error  $\|\varphi^e - \varphi^a\|/\|\varphi^e\|$  is used, where  $\varphi_i^e$  is the exact solution at node  $i$  and  $\varphi_i^a$  is the approximate solution at node  $i$ . Several features are apparent. First, the accuracy of the approximate solution

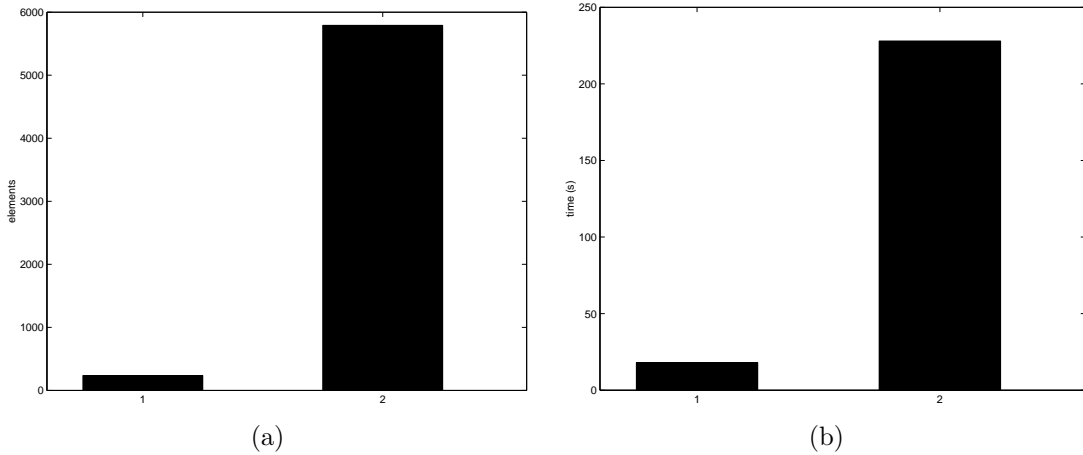


Figure 3: (a) Number of elements needed in mesh for comparable accuracy. (b) Time taken for comparable accuracy. 1: RBFs (no boundary information). 2: Shape functions.

diminishes as the ratio  $D_{yy}/D_{xx}$  is increased. This is in agreement with the observation that the problem is most difficult numerically when this ratio is large. Second, the accuracy of the radial basis function-based methods is much better than that offered by the method of shape functions. Third, the inclusion of boundary information in the RBF-based iterations is beneficial, giving typically an order of magnitude increase in the accuracy of the solution.

The increased accuracy offered by the radial basis function-based methods is not without cost. Each iteration involving radial basis functions takes significantly more time than those that use shape functions. Figure 2(b) compares the cumulative time taken to reach a solution after each stage. It is evident from the graph that employing radial basis functions results in a much longer execution time than when using shape functions alone. In this time however, a much more accurate solution is generated. Figure 3(a) shows the number of elements needed in the mesh for shape functions alone to generate a solution of comparable accuracy to radial basis functions in the case where  $D_{yy}/D_{xx} = 1000$ . Figure 3(b) shows the time taken to generate this solution. It is evident that using radial basis functions allows accurate solutions to be generated in much less time than by using shape functions alone.

## 7 Conclusions

The use of radial basis functions along with three-point Gaussian quadrature in the discretisation of the finite volume method can yield accurate solutions on a much coarser mesh than is possible when using shape functions. This approach is well-suited

for steady-state diffusion problems, and can be incorporated into a Newton-Krylov method for solving nonlinear partial differential equations. The use of the method as a corrector to the method of shape functions is advantageous in that it allows for an accurate solution with fewer nonlinear iterations, and for efficient preconditioning by re-using information from the shape function-based iterations.

## References

- [1] K. Burrage and J. Erhel. On the performance of various adaptive preconditioned GMRES strategies. *Numerical Linear Algebra with Applications*, 5(2):101–121, 1998.
- [2] B. Carpentieri, I. S. Duff, and L. Giraud. Sparse pattern selection strategies for robust frobenius-norm minimization preconditioners in electromagnetism. *Numerical linear algebra with applications*, 7(7–8), 2000.
- [3] R.D. Cook. *Concepts and applications of finite element analysis*. Wiley, 2001.
- [4] J.F. Epperson. *An Introduction to Numerical Methods and Analysis*. Wiley, 2002.
- [5] B. Fornberg, T.A. Driscoll, G. Wright, and R. Charles. Observations on the behavior of radial basis function approximations near boundaries. *Computers & Mathematics with Applications*, 43(3-5):473–490, 2002.
- [6] P. Jayantha and I.W. Turner. A new higher order control-volume finite-element least-squares strategy for simulating transport in highly anisotropic media. Submitted to *Journal of Computational Physics*, 2002.
- [7] M.N. Özışik. *Heat Conduction*. Wiley, 1980.
- [8] R. Morgan. GMRES with deflated restarting. *SIAM J. Sci. Comput.*, 24(1):20–37, 2002.
- [9] M. Powell. *The theory of radial basis function approximations in 1990*, in Advances in Numerical Analysis, Vol. II: Wavelets, Subdivision Algorithms and Radial Basis Functions, pages 105–210. Oxford University Press, 1990.